International Journal of Mechanical, Industrial and Aerospace Sciences
ISSN: 2517-9950
Vol:14, No:9, 2020

Clean Sky 2 – Project PALACE: Aeration's Experimental Sound Velocity Investigations for High-Speed Gerotor Simulations

Benoît Mary, Thibaut Gras, Gaëtan Fagot, Yvon Goth, Ilyes Mnassri-Cetim

***Abstract*—**A Gerotor pump is composed of an external and internal gear with conjugate cycloidal profiles. From suction to delivery ports, the fluid is transported inside cavities formed by teeth and driven by the shaft. From a geometric and conceptional side it is worth to note that the internal gear has one tooth less than the external one. Simcenter Amesim v.16 includes a new submodel for modelling the hydraulic Gerotor pumps behavior (THCDGP0). This submodel considers leakages between teeth tips using Poiseuille and Couette flows contributions. From the 3D CAD model of the studied pump, the "CAD import" tool takes out the main geometrical characteristics and the submodel THCDGP0 computes the evolution of each cavity volume and their relative position according to the suction or delivery areas. This module, based on international publications, presents robust results up to 6 000 rpm for pressure greater than atmospheric level. For higher rotational speeds or lower pressures, oil aeration and cavitation effects are significant and highly drop the pump's performance. The liquid used in hydraulic systems always contains some gas, which is dissolved in the liquid at high pressure and tends to be released in a free form (i.e. undissolved as bubbles) when pressure drops. In addition to gas release and dissolution, the liquid itself may vaporize due to cavitation. To model the relative density of the equivalent fluid, modified *Henry's* law is applied in Simcenter Amesim v.16 to predict the fraction of undissolved gas or vapor. Three parietal pressure sensors have been set up upstream from the pump to estimate the sound speed in the oil. Analytical models have been compared with the experimental sound speed to estimate the occluded gas content. Simcenter Amesim v.16 model was supplied by these previous analyses marks which have successfully improved the simulations results up to 14 000 rpm. This work provides a sound foundation for designing the next Gerotor pump generation reaching high rotation range more than 25 000 rpm. This improved module results will be compared to tests on this new pump demonstrator.

***Keywords*—**Gerotor pump, high speed, simulations, aeronautic, aeration, cavitation.

I. Introduction

GEROTOR pumps are often use in industries to provide high pressure in hydraulic systems, or in lubrification systems including aeronautical applications. In this aeronautical environment, the oil tank pressure might be as low as atmospheric pressure (like 0.15 bar at 55 000 feet altitude) to higher than ground atmospheric pressure. The decrease in static pressure, due either to the ambient pressure and the high velocity inside the pump, causes cavitation and degassing. Both phenomena cause gas to appear in the fluid and may reduce the filling capability of pump and limit the flow rate. To avoid these phenomena, operational range of most of pumps is limited to 8 000 rpm, even if connected to a mechanical drive system with a gear reducer. Embracing the objectives of increasing durability and reducing weight, the European Clean Sky PALACE project develops a new pump's architecture directly connected to a turbine to rotate over 26 000 rpm. To design a predictable model, experiments reaching 14 000 rpm in conjunction with numerical simulations have been conducted with a conventional pump.

Work carried out by Gamez-Montero [1] highlighted the interest of gerotor over the last decade. Regarding phenomena of degassing and cavitation, few researchers have addressed the problem in gerotor pumps. Buono et al. [2], [3] and Shah et al. [4] attempt to model cavitation from physical modeling and experimental approach on a specific gerotor. To address cavitation prediction, first one uses the commercial software GT-SUITE, whereas the second one applies the submodel 'Generic Hydraulic System' on Amesim environment based on works from Pellegri et al. [5], [6]. Furthermore, Buono et al. [2], [3] make use of a vibration technique to observe cavitation conditions. Hydraulic test bench including calibrated orifices installed on suction and delivery ports of the pump are used to force the cavitation. These studies provide a step forward to a better understanding and prediction of aeration and cavitation in gerotor pumps. Most recently, Singh et al. [7] employed a modified version of the cavitation model published in the literature to enhance effect of dissolved and undissolved gas in PumpLinx environment. Less than 5% of inaccuracy was stated by authors for the comparison with the experimental data. Each of these studies has been conducted with rotational speed under 6 000 rpm and most of them use value of gas content from literature. In the following, three methods used to determine the value of occluded gas in oil are outlined.

The first method called AIR-X used an on-line lubricant aeration [8]-[11]. The operating principle is based on an accurate density measurement using X-ray transmission. An oil sample coming from the mechanical system is circulated continuously into a compact measuring chamber where the density measurement is performed.

Benoît Mary is Hydraulic Design Engineer, Gaëtan Fagot is Thermal & Hydraulic engineer, and Ilyes Mnassri is CFD Engineer for CETIM, Nantes, France (e-mail: benoit.mary@cetim.fr, gaetan.fagot@cetim.fr, Ilyes.mnassri@cetim.fr).

Thibaut Gras is Vibro-Acoustic Engineer and Yvon Goth is Vibro-Acoustic, Mechanical and Turbomachines Expert for CETIM, Senlis, France (e-mail: Thibaut.gras@cetim.fr, yvon.goth@cetim.fr).

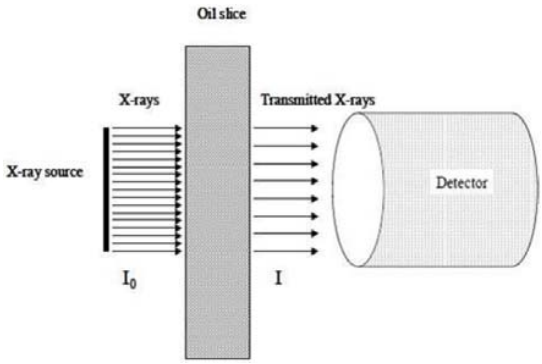

Fig. 1 Density measurement through X-Ray attenuation [12]

The second method consists of evaluating the amount of gas that could be dissolved in oil by controlling the volume inside a piston chamber. Zhou [13] compares CFD models with dynamic measurements. With this method, fluid density and bulk modulus have been specified. By integrating a simplified transport equation for the vapor and free air phases, the model is suitable to describe the main dynamic features of both cavitation processes (air release and vaporization) according to simple control volume approaches, commonly used to describe fluid power components or systems. Most recently, Kratschun [14] calculated Bunsen coefficients for three different hydraulic oils based on experimental results. Test ring consists of a chamber under piston compression filled with a mixture of hydraulic oil and air.

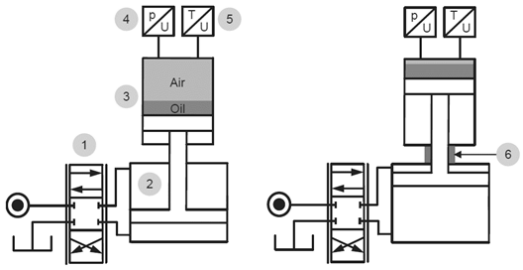

Fig. 2 Test rig operation [14]

The third method explores the sound velocity measurement in fluid medium at different pressure values. Thus, by comparison with analytic method it is possible to define the amount of undissolved gas. It can be estimated using the time delay of two emitter-receiver transducers. However, measurement issues can arise for large variations of the sound velocity which is expected in gas/liquid mixtures, that is why, the three sensors method seems to be more appropriate. This method developed by Margolis and Brown [15] allows to estimate the sound speed in a straight pipe using the spectral signals of the three sensors. It can be used without any external excitation so the existing hydroacoustic sources (pump, valves, …) are sufficient to calculate the sound speed.

Although the Air-X acquisition method has the advantage of directly providing the volumetric rate of degassing air, it requires a significant investment. The second method provides air content in a static way, without oil flow; therefore it cannot be representative of test line impacts. The third method, based on sound measurement, will be considered in following experiments because it takes account of test bench effects as confined gas bubbles into dead zones, and has a limited cost than X-ray analysis.

II. Experimental Setup

This part deals with a discussion about the test bench, then sound measurement will be highlighted according to the state of the art followed by the estimation of desorbed gas mass fraction.

A. Test Bench

A specific test bench (Fig. 3) has been set up to measure the sound speed inside the oil, contained in the upstream circuit. The test facility (Fig. 3) presented through the combination of several components is made of: the Gerotor pump (n1) driven by an electrical motor (n2), an oil tank (n3) and a straight pipe (n4) including three dynamic pressure sensors. The tank upstream from the pump has a free surface and contains a temperature probe. A static pressure sensor is mounted downstream from the pump. Pressure inside the upstream circuit can be decreased using a regulation valve (n5) and monitored by a vacuum gauge (n6). The oil volume flow rate is adjusted according to the pump rotational speed.

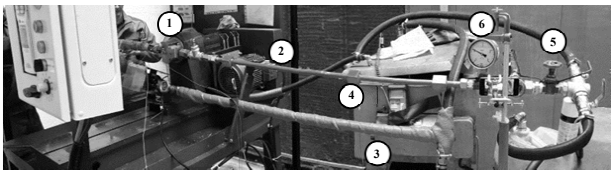

Fig. 3 Test bench

In order to visualize the flow and the occluded gas occurring when the pressure drop, a viewing window has been set up downstream from the valve (Fig. 4). Slow motion records and a back flashlight have been employed to improve the visualization and get a clear analyze of the bubble density.

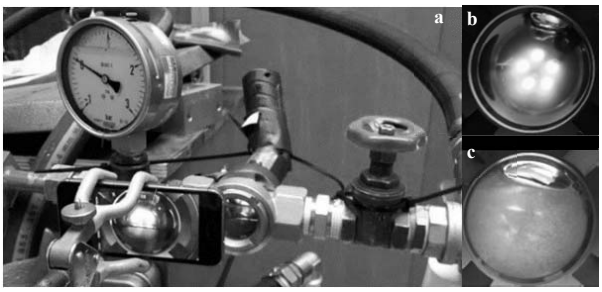

Fig. 4 (a) Viewing window downstream from the valve (b) flow at P = -0.1 barg (c) flow at P = -0.3 barg

The parietal dynamic pressure sensors have been set up in a straight measuring pipe of internal diameter 16 mm. The distance between the sensor named P_1 and P_2 is set to 330 mm

(Fig. 5), the distance between the sensor P_2 and P_3 is set to 660 mm. The sensor P_2 is considered as the reference sensor.

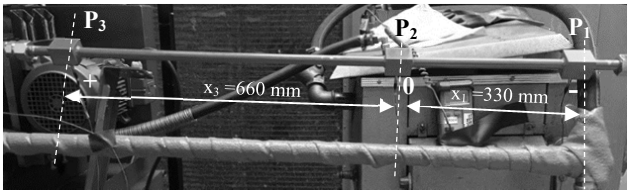

Fig. 5 Pressure sensor positions

B. Sound Speed Measurement

As seen in the test bench, the three sensors P_1, P_2 and P_3 of the straight pipe record the evolution of the pressure fluctuations due to the travelling of a plane wave sketching the sound speed measurement. In this study, the viscous effects have been neglected and the mean flow velocity is assumed to be much lower than the celerity of the waves.

According to the previous hypothesis, the pressure fluctuation can be written as:

$$P(x,t) = \alpha e^{j(\omega t+kx)} + \beta e^{j(\omega t-kx)} \quad (1)$$

$P(x,t)$ is the pressure fluctuation at position x, $k = \omega/c$ is the wavenumber, ω is the pulsation and c the sound speed of the waves in the pipe. This equation can be written in the frequency domain as:

$$P(x,f) = A\cos(kx) + B\sin(kx) \quad (2)$$

By applying this equation to the three positions $= -x_1$, $x = 0$ and $x = x_3$, one can find:

$$\begin{aligned} P_1 &= P(-x_1,f) = A\cos(kx_1) - B\sin(kx_1) \\ P_2 &= P(0,f) = A \\ P_3 &= P(x_3,f) = A\cos(kx_3) + B\sin(kx_3) \end{aligned} \quad (3)$$

By combining previous equations

$$P_1 \sin(kx_2) + P_3 \sin(kx_1) = P_2 \sin(k(x_1+x_2)) \quad (4)$$

Thus, by using transfer functions with P_2 as the reference sensor

$$P_{12} \sin(kx_2) + P_{32} \sin(kx_1) = \sin(k(x_1+x_2)) \quad (5)$$

With P_{12} and P_{32} the transfer functions such as $P_{12} = P_1/P_1$ and $P_{32} = P_3/P_2$. In the case where $x_2 = 2x_1$, the previous equation can be simplified as

$$2P_{12}\cos(kx_1) + P_{32} = \cos(2kx_1) + 2\cos(kx_1)^2 \quad (6)$$

This simplified equation (6) permits avoiding the right term to be zero. The celerity is estimated thanks to this equation by minimizing a cost function between the measurements (left term) and the analytical expression (right term).

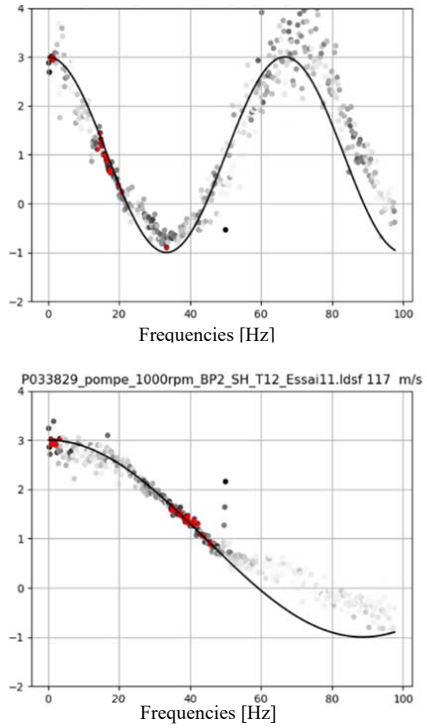

Fig. 6 Experimental curves against theoretical ones at: (a) 2000 rpm; P = -0.4 barg; c = 44m.s^{-1} (b) 1000 rpm; P = -0.1 barg; c = 117 m.s^{-1}

The sound speed measurement has been done for several operating points by varying both the downstream pressure and pump rotational speeds. Fig. 6 shows an example of superposed experimental and theoretical curves for different downstream pressure. As mentioned before, the cost function is minimized to find the speed of sound c in the pipe. It can be noticed that the algorithm only applies on spectral lines with coherence greater than 0.8 to limit measurement noise.

Fig. 7 highlights plots of the sound celerity in function of downstream pressure for all the operating points. The plotted circles survey different rotational speeds. The sound celerity increases as the downstream pressure gets higher.

Several theories have been proposed to explain this phenomenon; prior study comes with Jakobsen [16] who showed that the sound speed quickly decreases with an increase of low gas volume fraction in a liquid/gas mixture. It is due to interferences from released bubbles and sound waves. When the gas volume fraction becomes high enough, the interferences are reduced, and the speed of sound becomes close to the one in the gas.

In this experiment, when the downstream pressure decreases, air (released as bubbles in the oil) slowly increases the gas volume fraction and the sound speed in the oil/air mixture is also quickly reduced as shown in Fig. 7.

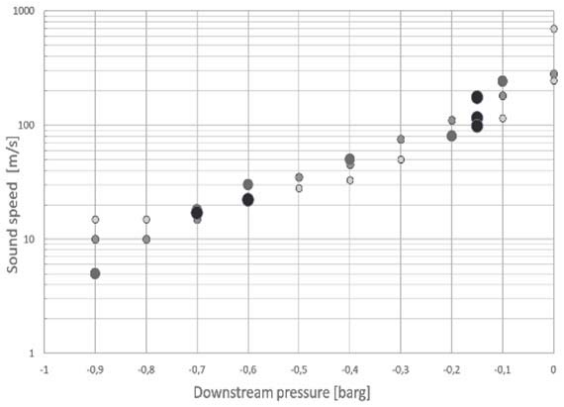

Fig. 7 Experimental sound speed against the downstream pressure for different rotational speeds

C. Test Desorbed Gas Mass Fraction Estimation

When the desorption phenomenon happens, the mixture needs equilibrium time to get back to equilibrium state after a pressure variation as described by [11], [13]. According to [17], this duration is not instantaneous, and it is compared to the fluctuation period. The first case known as frozen sound speed comes up when equilibrium time is longer than fluctuation period, so the desorbed quantity of gas does not vary while the wave front passes. In the other hand, when it is shorter, the mixture always gets back to equilibrium and we fall in the equilibrium sound speed case.

It is usually agreed that frozen conditions lead to a better estimation of the speed of sound [18]. Thus, the frozen model is used to estimate the sound speed in the mixture. The sound speed based on the gas mass fraction will be then compared with the sound speed of obtained with the three sensors method.

To simplify equations, the specific volume υ or mass volume is defined as

$$\upsilon = \frac{V}{m} = \frac{1}{\rho} \tag{7}$$

In a mixture of desorbed gas in a liquid, the specific volume of the liquid is noted υ_l and is considered as incompressible fluid (independent of the pressure variation) whereas, the gas specific volume $\upsilon_{g,P}$ is pressure dependent.

In the equilibrium state, the liquid contains dissolved gases, which vary with pressure. The dissolved gas mass fraction ϱ_0 can be expressed according to the solubility a_0 of air in the liquid as

$$\varrho_0 = a_0 \frac{\upsilon_l}{\upsilon_{g,P_0}} \tag{8}$$

Henry's law [19] states that the amount of dissolved gas in a liquid is proportional to its partial pressure above the liquid. Thus, it is possible to link the dissolved gas mass fraction ϱ from different pressure conditions (for example: atmospheric and reference) with this relation:

$$\frac{\varrho_0}{P_0} = \frac{\varrho_1}{P_1} \tag{9}$$

So, the desorbed gas mass fraction x in oil at pressure P can be written as

$$x = \varrho_0 (1 - \frac{P}{P_0}) \tag{10}$$

For the present mixture containing desorbed air in oil, the specific volume of the mixture υ_P at the pressure P can be derived from the air mass fraction as

$$\upsilon_P = (1 - x)\upsilon_l + x\upsilon_{g,P} \tag{11}$$

The specific volume of the gas at the pressure P can be deducted from the ideal gas law such as

$$\upsilon_{g,P} = \frac{P_0}{T_0}\frac{T}{P}\upsilon_{g,P_0} \tag{12}$$

In the air/oil mixture, the sound speed is given by the *Newton–Laplace* equation

$$c = \sqrt{K_s \upsilon_P} \tag{13}$$

with K_s the coefficient of stiffness such as

$$\frac{1}{K_s} = -\frac{1}{\upsilon_P}\left(\frac{\delta \upsilon_P}{\delta P}\right) \tag{14}$$

Therefore, sound celerity can be written as

$$\frac{1}{c^2} = -\frac{1}{{\upsilon_P}^2}\left(\frac{\delta \upsilon_P}{\delta P}\right) \tag{15}$$

Through algebraic manipulations, (15) becomes:

$$\frac{1}{c^2} = -\frac{1}{{\upsilon_P}^2}\left((1 - x)\frac{\delta \upsilon_l}{\delta P} + x\frac{\delta \upsilon_{g,P}}{\delta P} + (\upsilon_l - \upsilon_{g,P})\frac{\delta x}{\delta P}\right) \tag{16}$$

According to [17], the frozen model considers the mass fraction x as constant along the measuring pipe the previous equation is rewritten as:

$$\frac{1}{c^2} = -\frac{1}{{\upsilon_P}^2}\left((1 - x)\frac{{\upsilon_l}^2}{{c_l}^2} + x\frac{{\upsilon_{g,P}}^2}{{c_g}^2}\right) \tag{17}$$

where c_l and c_g refers to the sound speed inside the oil and the air at the operating temperature.

The following values are fixed for the numerical applications: sound speed in oil is taken as c_l = 1200 m.s^{-1}, in air c_g = 342 m.s^{-1}, solubility a_0 = 6.8%, υ_l= 1/940 m^3.kg^{-1} and υ_{g,P_0}= 1/1.2 m^3.kg^{-1}.

The solubility of air in the liquid a_0 was found by minimizing a cost function between the frozen model and the three sensors sound speed. Fig. 8 shows the sound speed values resulting from these two methods using the solubility a_0 = 6.8%. A good consistency is outlined from the two methods, which tends to validate the frozen model and the gas mass fraction in order to be able after that to evaluate the oil/ air mixture density.

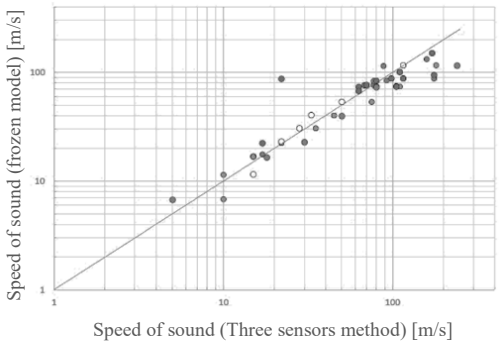

Fig. 8 Speed of sound obtained via the frozen model against speed of sound obtained via the three sensors method

The curve values on Fig. 9 represent the growth of the mixture density in function of downstream pressure that will be used as input data for the pump simulation. The density quickly decreases as downstream pressure, and when this pressure drop occurs, the gas volume fraction increases, and the associated density decreases.

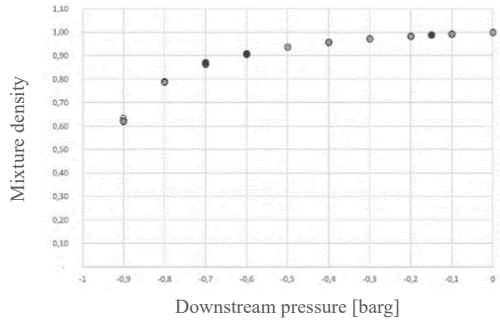

Fig. 9 Mixture density versus downstream pressure

III. Numerical Model

As Gamez-Montero et al. [20] show, the use of CFD in all fields of engineering is growing exponentially. Main difficulties with this tool consist of modelling dynamic mesh with contact points. The same authors [21] used ANSYS Fluent 12 to model the contact point as a high-density zone. This method was updated by Garcia-Vilchez [22] to increase robustness. Castilla at al. [23] used a similar model with OpenFOAM. To confront two kind of simulations Pellegri [5] benchmarks 1D Amesim - 3D PumpLinx model with a good agreement.

CFD investigations offered high degree details of internal pump flow with high computational time. So, 3D model looks more appropriate for advanced studies. Therefore, a 1D model as Amesim environment seems to be more suitable for this study.

A. Gerotor Configuration Tool

Amesim v16 contained a "submodel" to represent gerotor pump, called gerotor configuration tool [24] established from [25]-[27]. A set of 8 parameters are needed to model the gerotor pump (Figs. 10 and 11).

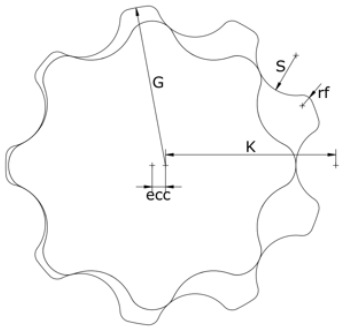

Fig. 10 Gears dimensions; z: number of teeth on external gear, H: gears thickness [mm], rotinit = shaft initial angle [degree]

Inlet and outlet ports can be modelled in two different ways. The analytic one considers an annular shape limited to an angular sector defined by the user. The other one can be specified as a table containing the coordinates (x, y) of points describing the contour of the port.

Each cavity trapped in the spaces between the teeth is modeled as a variable volume. For each control volume the flow rate going through the suction/delivery ports is computed with an orifice law with:

$$dm = \rho . c_q . A . \sqrt{\frac{2.|\Delta P|}{\rho}} \tag{18}$$

with: $c_q = c_{q\,max} . \tanh\left(\frac{2.\lambda}{\lambda_{crit}}\right)$, and: $\lambda = \frac{D_h}{v} . \sqrt{\frac{2.|\Delta P|}{\rho}}$

For this study, values for c_q and λ are set to 0.57 and 2 000 for suction port, and 0.29 and 1 000 for discharge port. These values remain in a reasonable range according to the authors' experience and literature data.

Only internal leakages between teeth tips of the internal and external gears are considered in the Amesim submodel as a sum of a *Poiseuille* and a *Couette* contribution as

$$qleakp = \frac{H.{h_{min}}^3}{12.\mu.L} \Delta P \tag{19}$$

$$qleakc = \frac{v_s.h_{min}.H}{2} \tag{20}$$

The gap h_{min} in Fig. 12 is fixed and equal to the clearance between the two rotors. The length L for *Poiseuille* calculation is determined as the distance between two regions in which the clearance between the rotors is equal to

$$h^* = h_{min} . (1 + \varepsilon) \tag{21}$$

According to [5], the value of ε is chosen to be 0.1. An analysis by analytic methods of the flow rate by the several leakage paths described by [26] has shown that internal leakages are predominant compared to the others.

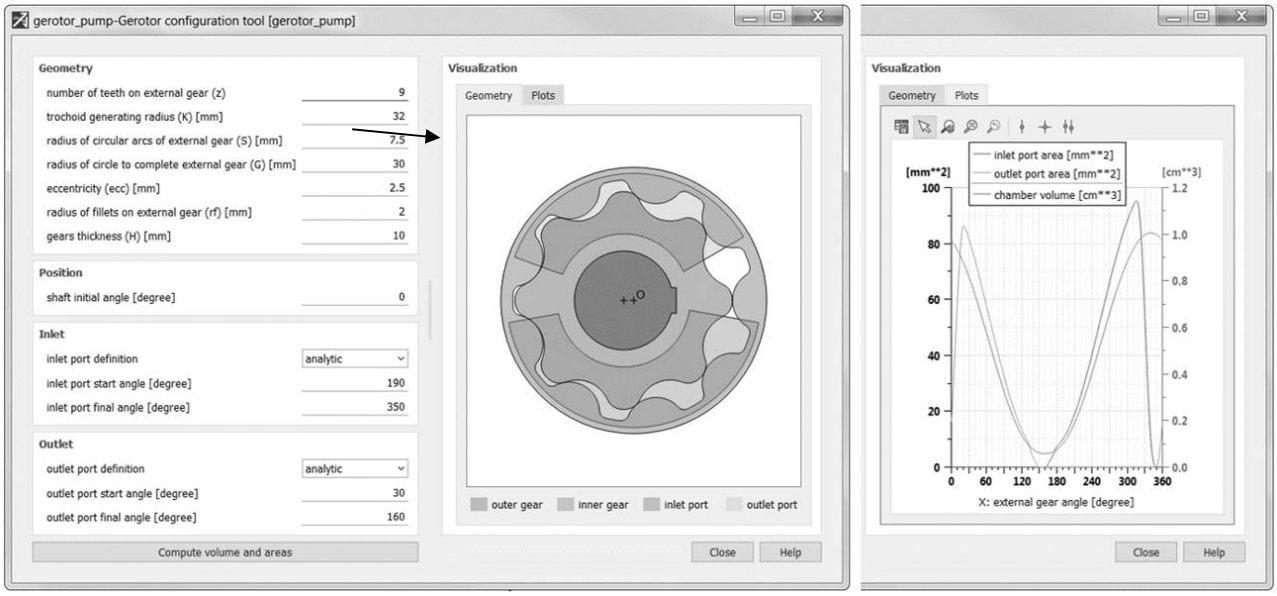

Fig. 11 Gerotor configuration tool

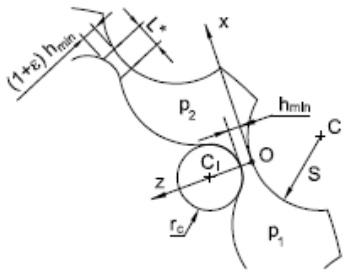

Fig. 12 Internal gap in gerotor pumps [28]

B. Aeration/Cavitation Modelling

The liquid used in hydraulic systems always contains some gas, generally air dissolved in the liquid. When the pressure drops, it tends to be released in a free form (bubbles): this process is called aeration. Conversely if the pressure rises the free gas tends to dissolve again in the liquid (dissolution).

In addition to air release and dissolution, the hydraulic liquid itself may vaporize due to cavitation (pressure decrease) or boiling (temperature increase). The cavitation phenomenon is important to obtain a realistic behavior in thermal-hydraulic capacitances at low pressure.

The situation is summarized on Fig. 13:

- Above P_{sat}, the gas is dissolved in the liquid in a molecular form. The gas molecules do not increase the volume of the liquid although they do increase its mass. The compressibility of the liquid is not changed by the presence of the dissolved gas. Below P_{sat}, gas bubbles appear, changing the bulk modulus of the equivalent fluid which is now a mixture.
- Vapor bubbles appear when pressure becomes smaller than P_{vaph}. As gas bubbles, they significantly change the bulk modulus of the mixture. Below P_{vapl}, there is no more liquid in the mixture.

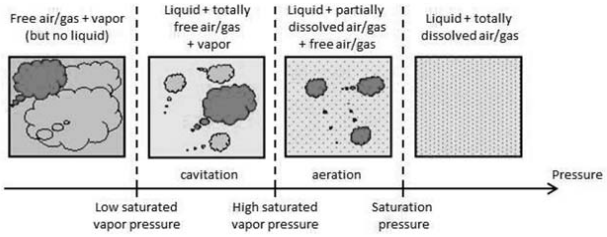

Fig. 13 Fluid states

Vaporization pressure, e.g. P_{vapl} has been evaluated in laboratory between 70 and 170 °C and interpolated for other values. It should be noted that the vaporization pressure values are considerably low (< 0.1 mbar). This analysis permits to increase knowledge of oil properties that will be implemented in Amesim's fluid database.

P_{vaph}, P_{sat} and the amount of oil's gas content *Aeration* are usually estimated by parametric studies to correlate performances curves obtained from tests results. This kind of study requires some computational time and the set of values acquired may not be representative of oil's characteristics.

Table I exposes values of the aeration model computed with parametric study and the sound velocity analysis.

TABLE I
VALUES FOR AERATION MODELLING

Case	P_{vapl}	P_{vaph}	P_{sat}	*Aeration*
1 – Estimation	≈ 0.1 mbar	0.25 bar	1.5 bar	150 mg/kg
2 – Real Values	≈ 0.1 mbar	0.15 bar	1.3 bar	87 mg/kg

It can be seen from the curve of Fig. 14 based on values from Table I that equivalent density worked out from real values compares well with measurement data. Starting from atmospheric pressure, measurement and the both simulations' data are perfectly superposed and reach an asymptotic value as

pressure increases.

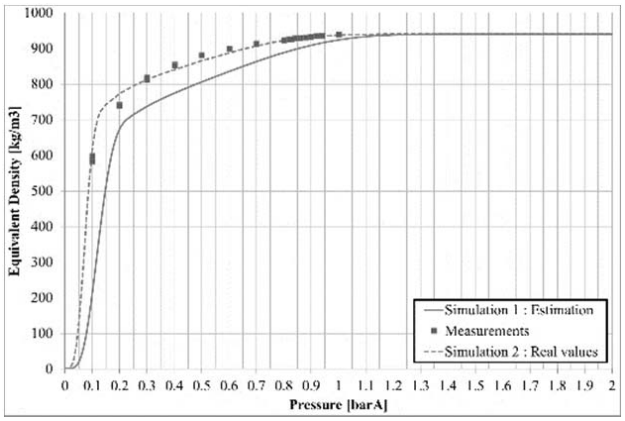

Fig. 14 Equivalent density

C. System Simulation

Fig. 15 presents the Amesim model scheme based on the test bench used to determinate aeration rate.

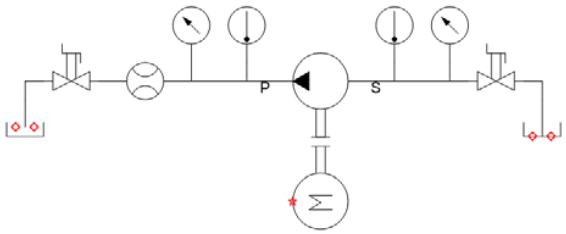

Fig. 15 Schematic representation of test ring

A specific batch is set to cover the whole range of test cases from low to high velocities and from low to high delivery and suction pressure. To compare simulation results and measurements, a specific python code is employed to extract mean values of pressure and flow rate for the last pump revolution.

IV. Results Analysis

This section explores the results performed by simulation 1 (from parametric study) and simulation 2 (from sound celerity analysis). Figs. 16 and 17 exhibit performance curves in function of rotational velocity, for the two simulations data at atmospheric pressure and pressure difference evolution at 6 000 rpm.

The simulation based on real values is closer to measurements with a 5% difference compared to simulation with estimated values. The last ones performed results with more disparity but remains under 20%. It can be also noted in Fig. 16 that as the rotational velocity increases, the gap with the performance curves is more pronounced.

Only one set of simulations was necessary to obtain results shown in Fig. 17. The Amesim inputs are specified as Real Values from Table I. The results are much closer to the test measurements with a difference less than 5%.

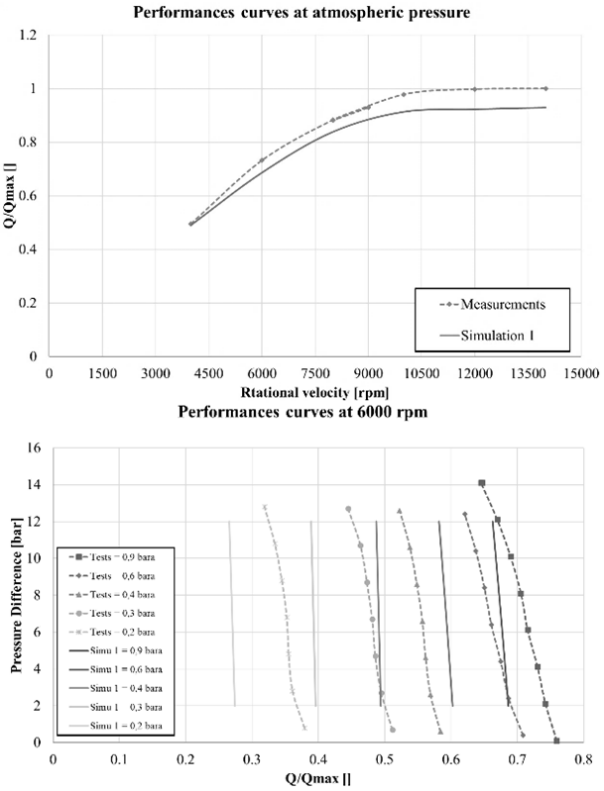

Fig. 16 Performance curves – Comparison tests and simulation 1

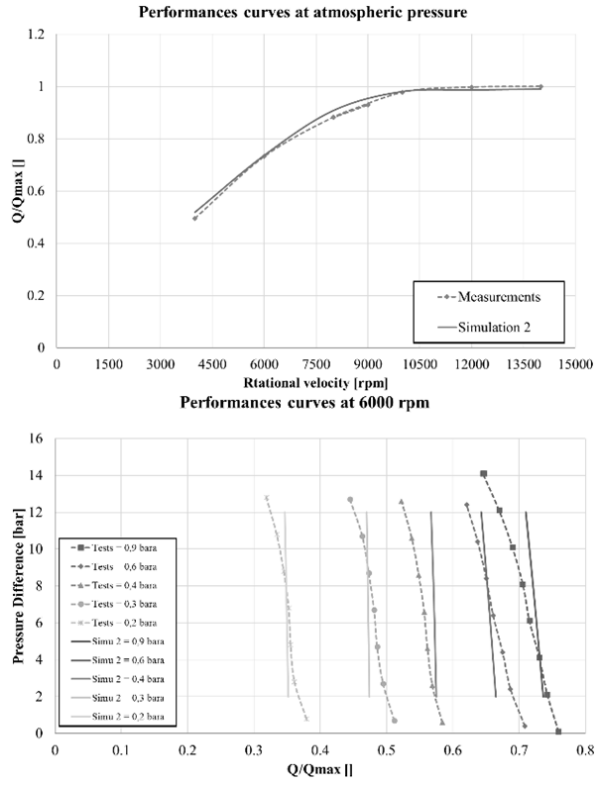

Fig. 17 Performances curves – Comparison tests and simulation 2

On all curves, it is worth to note that from atmospheric pressure the performance is constant at certain value and especially shows no dependencies to the rotational velocity till 14 000 rpm. After this value, degassing and cavitation might be predominant and flow rate theoretically should decrease.

Considering the three-sensor method allows to directly define the main oil properties into the Amesim fluid database. Thanks to this method, the Gerotor model is more predictive at high-speed and low-pressure operating conditions.

V. Conclusions

A complete three-sensor method investigation of the evolution of gas contained in oil in function of pressure by a sound velocity analysis has been processed. Results from this investigation have been supplied in Amesim model. The low cost three-sensor method is helpful to determinate the set of aeration model parameters and consequently improves the Amesim model prediction.

Further tests will be carried out on a high-speed pump prototype in operational conditions (low pressure, high speed up to 26 000 rpm). This will be an opportunity to confirm the experimental and numerical studies. Developing dynamics effects of degassing and dissolution as explained by Rundo [11] presents a way to improve Amesim model.

Acknowledgment

The CETIM team warmly thanks our industrial partner into PALACE consortium (SERV) to have allowed these experiments on their facilities and for their confidence into CETIM.

The project leading to this application has received funding from the Clean Sky 2 Joint Undertaking under the European Union's Horizon 2020 research and innovation program under Grant Agreement No 785293.

References

[1] Gamez-Montero P-J., Codina E., Castilla R., "A Review of Gerotor Technology in Hydraulic Machines", Energies. 12 (2019), 2423

[2] Buono D., Schiano di Cola F.D., Senatore A., Frosina E., Buccilli G., Harrison J., "Modelling approach on a Gerotor pump working in cavitation conditions", Energy Procedia 2016, 101, 701–709.

[3] Buono D., Siano D., Frosina E., Senatore A., "Gerotor pump cavitation monitoring and fault diagnosis using vibration analysis through the employment of auto-regressive-moving-average technique" Simul. Model. Pract. Theory 2017, 71, 61–82.

[4] Shah Y.G., Vacca A., Dabiri S., Frosina E., "A fast lumped parameter approach for the prediction of both aeration and cavitation in Gerotor pumps. Meccanica 2017, 53, 175–191.

[5] Pellegri M., Vacca, M., Frosina E., Buono D., Senatore, A., "Numerical analysis and experimental validation of Gerotor pumps: A comparison between a lumped parameter and a computational fluid dynamics-based approach", Proc. Inst. Mech. Eng. C 2016, 231, 4413–4430.

[6] Pellegri M., Vacca A., Devendran R., Dautry E., Ginsberg B., "A Lumped Parameter Approach for GEROTOR Pumps: Model Formulation and Experimental Validation", In Proceedings of the 10th International Fluid Power Conference, Dresden, Germany, 8–10 March 2016.

[7] Singh R., Salutagi S.S., Piotr P., Madhavan J., "Study of Effect of Air Content in Lubrication Oil on Gerotor Pump Performance Using CFD Simulations", SAE Technical Papers 2019-26-0300, SAE International: Warrendale, PA, USA, 2019, pp. 1–5.

[8] Baran B., and Chen, W., "Assessing the Windage Tray Blockage Effect on Aeration in the Oil Sump", SAE Technical Paper 2007-01-4109.

[9] Ippoliti L., Steime, J., Hendrick P., "Investigation on an Oil Aeration Measurement Technique for the Study of Pump Performance in an Aircraft Engine Lubrication System", Proceedings of the ASME Turbo Expo 2015: Turbine Technical Conference and Exposition. Volume 5C: Heat Transfer, 2015.

[10] Ippoliti L., Vincké J., Hendrick P., "Oil Aeration and Degassing Measurements for the Study of Aero-Engine Oil Pump Performance in Cavitation", Proceedings of the ASME 2017 Fluids Engineering Division Summer Meeting, Volume 1A, Symposia, 2017.

[11] Rundo M., Squarcini R., Furno F., "Modelling of a Variable Displacement Lubricating Pump with Air Dissolution Dynamics", SAE Int. J. Engines 11(2):2018.

[12] DSi, "Air-X – On-line Lubricant Aeration – Technical Brochure", 2018

[13] Zhou J., Vacca A., Manhartsgruber B., "A Novel Approach for the Prediction of Dynamic Features of Air Release and Absorption in Hydraulic Oils", ASME. J. Fluids Eng. September 2013; 135(9): 091305.

[14] Kratschun F., Schmitz K., Murrenhoff, H., "Experimental investigation of the Bunsen and the Diffusion coefficients in hydraulic fluids", 10th International Fluid Power Conference, March 8 - 10, 2016, Vol. 1, pp. 181-192.

[15] Margolis D.L., Brown F.T., "Measurement of the propagation of long-wavelength disturbances trough turbulent flow in tubes," *J Fluids Eng*, pp. 70–78, 1976.

[16] Jakobsen J.K., "On the mechanism of head breakdown in cavitating inducer". *J Basic Eng Trans ASME* 291–305, 1964.

[17] Resler E.L, "Characteristics and sound speed in nonisentropic gas flows with nonequilibrium thermodynamic states". *Journal of the Aeronautical Sciences*, 24(11), 785-790, 1957.

[18] R. Sedney, J.C South, and N Gerber, and U.S. Army Ballistic Research Laboratory "Characteristic Calculation of Non-equilibrium Flows", Ballistic Research Laboratories, 1962

[19] Henry W., "Experiments on the quantity of gases absorbed by water, at different temperatures, and under different pressures", *Philosophical Transactions of the Royal Society of London*, vol. 93, p. 29–274, 1803.

[20] Gamez-Montero P.J.; Codina E.; Castilla R., "A Review of Gerotor Technology in Hydraulic Machines", Energies 2019, 12, 2423.

[21] Gamez-Montero P.J., Castilla R., Del Campo D., Ertürk N., Raush R., Codina E., "Influence of the interteeth clearances on the flow ripple in a gerotor pump for engine lubrication", Proceedings of the Institution of Mechanical Engineers, Part D: Journal of Automobile Engineering 2012 226: 930.

[22] Garcia-Vilchez M., Gamez-Montero P., Codina, E., Castilla R., Raush G., Freire V., Francisco J., Ri, C., "Computational fluid dynamics and particle image velocimetry assisted design tools for a new generation of trochoidal gear pumps", Advances in Mechanical Engineering. 7, 2015.

[23] Castilla, R., Gamez-Montero, P. J., Raush, G., and Codina, E., "Method for Fluid Flow Simulation of a Gerotor Pump Using OpenFOAM", ASME. J. Fluids Eng. November 2017.

[24] Siemens PLM, "LMS Imagine.Lab AMESim Thermal-Hydraulic Component Design Manual", 2017.

[25] Fabiani, M., Mancò, S., Nervegna, N., Rundo, M. et al., "Modelling and Simulation of Gerotor Gearing in Lubricating Oil Pumps", SAE Technical Paper 1999-01-0626, 1999.

[26] Mancò S., Nervegna N., Rundo M., Armenio G., Pachetti C., Trichilo R. "Gerotor Lubricating Oil Pump for IC Engines", SAE Transactions - Journal of Engines (1998). 107. 2267-2283.

[27] Ivanovic L., Josifovic D., Blagojevic M., Stojanovic B., Ilic A., "Determination of gerotor pump theoretical flow", COMETa, 2012.

[28] Rundo M., "Models for Flow Rate Simulation in Gear Pumps: A Review", In: ENERGIES, vol. 10 n. 9 (2017), 1261, - ISSN 1996-1073.